The Low energy structure of the Nucleon-Nucleon interaction: Statistical vs Systematic Uncertainties

R. Navarro Pérez

Departamento de Física Atómica, Molecular y Nuclear and Instituto Carlos I de Física Teórica y Computacional
Universidad de Granada, E-18071 Granada, Spain.

Department of Physics and Astronomy, Iowa State University, Ames, Iowa 50011, USA.

J.E. Amaro

Departamento de Física Atómica, Molecular y Nuclear and Instituto Carlos I de Física Teórica y Computacional
Universidad de Granada, E-18071 Granada, Spain.

E. Ruiz Arriola

Departamento de Física Atómica, Molecular y Nuclear and Instituto Carlos I de Física Teórica y Computacional
Universidad de Granada, E-18071 Granada, Spain.

Abstract

We analyze the low energy NN interaction by extracting threshold parameters uncertainties from the coupled channel effective range expansion up to $j \leq 5$. This is based on the Granada-2013 database where a statistically meaningful partial wave analysis comprising a total of 6713 np and pp published scattering data from 1950 till 2013 below pion production threshold has been made. We find that for threshold parameters systematic uncertainties are generally at least an order of magnitude larger than statistical uncertainties.

1. Introduction

The NN interaction has traditionally been inferred from pp and np scattering data. This task is hampered both by the fragmentary body of experiments as well as by the incomplete status of the models used to analyze them. These aspects have important consequences regarding the predictive power, accuracy and precision in theoretical nuclear physics. In this paper we will restrict the analysis to the NN scattering amplitude and try to set lower bounds both on statistical as well as systematic uncertainties in the long wavelength limit where model details should become least relevant. A major finding of our present work, which comes as a surprise, is that even in the low energy limit the systematic uncertainties dominate over those statistical uncertainties arising directly from the same experimental data.

The low energy structure of the NN interaction has received a recurrent attention since the late 40's when Bethe proposed the effective range expansion [1]. The shape and model independence of the amplitude captured with a few number of parameters the essence of the NN force; an unique and particularly appealing universal pattern in the long wavelength limit of short range interactions. Because this is a low energy expansion of the full scattering amplitude in powers of small momentum, higher partial waves are needed and one may imagine an ideal situation with a direct determination from low energy scattering only. However, these data are scarce and in reality a much higher accuracy can be obtained by intertwining lower and higher energies via a large scale Partial Wave Analysis (PWA) so that many more data contribute to the threshold parameters precision. This interrelation cannot be achieved for free, since as we discuss next some unavoidable model dependence is introduced, thus generating a source for systematic errors beyond the genuine statistical errors of the PWA.

Indeed, the NN scattering amplitude contains 10 independent functions of energy and angle and a complete set of experiments is needed to determine it without model dependence [2]. While the usefulness of polarization was soon realized [3] as well as the strong unitarity constraints on the uniqueness of the solution [4, 5] (see [6] for an analytical solution), complete sets of measurements are scarce at the energies relevant to nuclear structure applications, corresponding to energies below pion production threshold. As a consequence a PWA in conjunction with the standard least squares χ^2-method is usually pursued and a set of measured scattering observables at given *discrete* energy and angle values are fitted. This incomplete and discretized experimental information requires using smooth interpolating energy dependent functions for the scattering matrix in all partial waves for nearby but unmeasured kinematic regions. Alternatively, quantum mechanical potentials with proper long distance behavior generate analytical energy dependence with the adequate cut-structure in the complex energy plane. This

approach is subjected to inverse scattering off-shell ambiguities [7] as the potential contains generically 10 matrix functions [8], manifesting themselves as a systematic uncertainty in the observables at the interpolated, not directly measured, energy values. If one fixes a maximum energy for the PWA the ambiguities reflect the finite spatial resolution corresponding to the shortest de Broglie wavelength below which the interaction is not determined by the data. Thus, we might expect that in the long wavelength limit systematic uncertainties will be greatly reduced. Our work can be framed within the currently growing efforts to realistically pin down the existing uncertainties stemming from different sources in nuclear physics [9, 10]. An upcoming special issue dedicated to this topic is scheduled to appear in Jour. Phys. G [11] by February 2015.

2. Data, Models and Uncertainties

The description of NN scattering data by phenomenological potentials started in the mid-fifties [12] and has been pursued ever since (see [13] and references therein for a pre-nineties review). However a successful fit, determined by the merit figure χ^2/d.o.f ~ 1, was not achieved until 1993 when the Nijmegen group applied in this context the long established Chauvenet's 3σ criterion (see [14]) to statistically reject data with an improbably high or improbably low χ^2 value [15]. After this, several potentials describing data up to a laboratory frame energy of 350 MeV were developed with similar χ^2/d.o.f values. All of them include the distinguished charge dependent one pion exchange (OPE) as the long range part of the interaction, and around 40 parameters for the short and intermediate range regions [15, 16, 17, 18, 19]. These OPE-tailed potentials with χ^2/d.o.f $\lesssim 1$ have played a major role in nuclear physics. In a recent paper we have updated the PWA by including data up to 2013, improving after [19] the 3σ criterion to select a self-consistent database with $N = 6713$ np and pp scattering data and providing statistical error bars to the fitting parameters [20, 21]. The delta-shell (DS) representation of the potential allowed the propagation of statistical uncertainties from the scattering data into potential parameters, phase shifts, scattering amplitudes and deuteron properties. This was possible due to the simplification in calculating the Hessian matrix. Subsequently, we have extended DS potential including chiral two pion exchange (χTPE) in the intermediate and long range regions [22, 23]. We also introduced a local and smooth potential parameterized as a sum of Gaussian functions with OPE [24]. Our potentials incorporate the appropriate propagation of statistical uncertainties. This has been possible because the residuals of our fits are a precisely normal distributed data set. This requirement of the χ^2 method, has been verified *a posteriori* with a high confidence level. We stress that a lack of normality in the residuals would strongly suggest the presence of systematic uncertainties in the analysis, disallowing the propagation of statistical errors. In our case, where normality is unequivocally fulfilled, we have propagated statistical uncertainties by applying the bootstrap Monte Carlo method *directly* to the experimental data [26], which simulates an ensemble of conceivable experiments based on the experimental uncertainties estimates.

A similar method has successfully been applied to estimate the statistical uncertainty in the triton binding energy [27].

3. Low energy expansion

As already mentioned, in the absence of complete sets of measurements one must resort to potentials to carry out the PWA. Since the form of the potential is chosen and fixed *a priori*, the analysis of NN scattering data is subjected to inverse scattering ambiguities which are amplified as the energy increases. Therefore one expects lowest energy information to be more universal and thus we use the effective range expansion (ERE) [1] as the suitable tool. Although for S-waves the calculation of the low energy threshold parameters is straightforward for NN potentials, their calculation for higher and coupled channel partial waves is a computational challenge. To start with, there are not even ready-to-use formulas in the coupled channel case, and actually a low energy expansion of the wave function to high orders is needed. In addition, higher partial waves become numerically unstable as the main contribution comes from very long distances requiring demanding numerical computations. This is the reason why these low energy parameters have been very rarely computed or when they have been a very limiting accuracy has been displayed. Using Calogero's variable phase approach to the full S-matrix [28] they have only been calculated for the Reid93 and NijmII potentials up to $j \leq 5$ [29]. Here we improve on the accuracy of that work and determine for the first time the statistical uncertainties of the low energy threshold parameters. The low energy parameters in higher partial waves determined in Ref. [29] found interesting applications. They have been used to implement renormalization conditions [30, 31, 32, 33] or to analyze causality bounds in np scattering [34].

In the well known case of central waves $^1S_0$ and $^3S_1$ the ERE is given by (taking nuclear bar phases)

$$k \cot \delta_0 = -\frac{1}{\alpha_0} + \frac{1}{2} r_0 k^2 + v_2 k^4 + v_3 k^6 + v_4 k^8 + \ldots, \quad (1)$$

where k is the center of mass momentum, δ_0 is the corresponding partial wave phase-shift, α_0 is the scattering length, r_0 is the effective range and v_i are known as the curvature parameters. The generalization to N-coupled partial waves with angular momenta $(l_1, \cdots, l_N)$ can be done by introducing the $\hat{\mathbf{M}}$ matrix defined as

$$\mathbf{D} \mathbf{S} \mathbf{D}^{-1} = \left(\hat{\mathbf{M}} + ik\mathbf{D}^2 \right) \left(\hat{\mathbf{M}} - ik\mathbf{D}^2 \right)^{-1}, \quad (2)$$

where $\mathbf{S}$ is the usual unitary S-matrix and $\mathbf{D} = \text{diag}(k^{l_1}, \ldots, k^{l_N})$. In the limit $k \to 0$ $\hat{\mathbf{M}}$ becomes

$$\hat{\mathbf{M}} = -\mathbf{a}^{-1} + \frac{1}{2}\mathbf{r}k^2 + \mathbf{v_2}k^4 + \mathbf{v_3}k^6 + \mathbf{v_4}k^8 + \ldots, \quad (3)$$

where $\mathbf{a}$, $\mathbf{r}$ and $\mathbf{v_i}$ are the coupled channel generalizations of α_0, r_0 and v_i respectively. Due to $n\pi$ exchange $\hat{\mathbf{M}}(k)$ has branch cuts at $k = \pm inm_\pi/2$, and thus the ERE converges for $|k| < m_\pi/2$ or $E_{\text{LAB}} \lesssim 10\text{MeV}$. Conversely, the ERE to *finite* order does
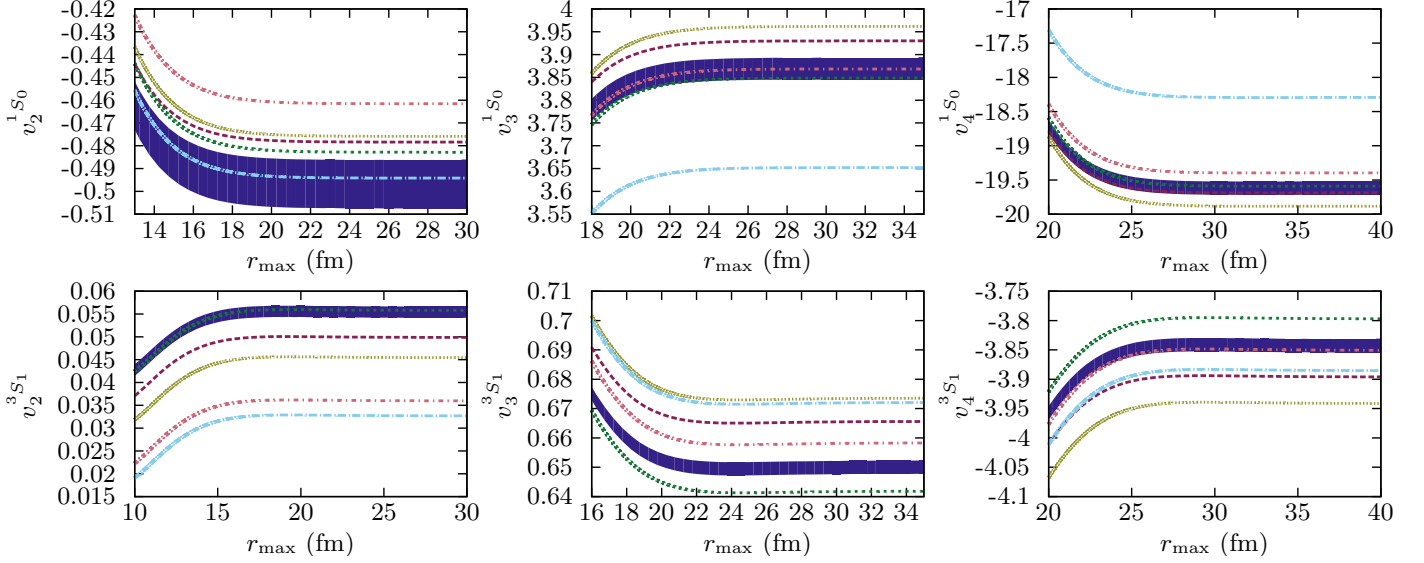
Figure 1: Convergence of the $^1S_0$ and $^3S_1$ low energy threshold parameters v_2, v_3 and v_4 as a function of the integration distance and for the DS-OPE [20, 21] (blue band), DS-χTPE [22, 23] (dashed red line), Gauss-OPE [24] (dotted green line), NijmII [16] (dotted yellow line), Reid93 [16] (dotted dashed light blue line) and AV18 [17] (dotted dashed light red line). The width of the blue band reflects our statistical error estimate.

not allow to reconstruct the full functions in the complex plane without the explicit cut structure information.

In the NN case these matrices have dimension 1 and 2. We refer to Ref. [29] for further details. In the interesting case of the $^3S_1$ eigen-channel, one has [1]

$$k \cot \delta_{3S1}^{\text{Eigen}} = -\frac{1}{\alpha_{3S1}^{\text{Eigen}}} + \frac{1}{2} r_{3S1}^{\text{Eigen}} k^2 + v_{3S1}^{\text{Eigen}} k^4 + \dots \quad (4)$$

where we get for the effective range parameters the relations between the eigen and the nuclear bar (denoted emphatically as barred) representations,

$$\alpha_{3S1}^{\text{Eigen}} = \bar{\alpha}_{3S1} \quad (5)$$

$$r_{3S1}^{\text{Eigen}} = \bar{r}_{3S1} + \frac{2\bar{r}_{E1}\bar{\alpha}_{E1}}{\bar{\alpha}_{3S1}} + \frac{\bar{r}_{3D1}\bar{\alpha}_{E1}^2}{\bar{\alpha}_{3S1}^2} \quad (6)$$

$$\begin{aligned} v_{3S1}^{\text{Eigen}} = {} & \bar{v}_{3S1} + \frac{1}{4}\bar{\alpha}_{3D1}\bar{r}_{E1}^2 \\ & + \frac{\bar{\alpha}_{E1}}{4\bar{\alpha}_{3S1}}\left(2\bar{\alpha}_{3D1}\bar{r}_{3D1}\bar{r}_{E1} - \bar{\alpha}_{E1}\bar{r}_{E1}^2 + 8\bar{v}_{E1}\right) \\ & + \frac{\bar{\alpha}_{E1}^2}{4\bar{\alpha}_{3S1}^2}\left(\bar{\alpha}_{3D1}\bar{r}_{3D1}^2 - 2\bar{\alpha}_{E1}\bar{r}_{3D1}\bar{r}_{E1} + 4\bar{v}_{3D1}\right) \\ & + \frac{1}{4\bar{\alpha}_{3S1}^3}\left(4\bar{\alpha}_{E1}^2 - \bar{\alpha}_{E1}^4\bar{r}_{3D1}^2\right) \end{aligned} \quad (7)$$

and so on.

4. The discrete variable-S-matrix method

The variable-$\hat{\mathbf{M}}(R, k)$ matrix equation is given by

$$\begin{aligned} \frac{\partial \hat{\mathbf{M}}(R, k)}{\partial R} = {} & \left(\hat{\mathbf{M}}(R, k)\mathbf{A}_k(R) - \mathbf{B}_k(R)\right)\mathbf{U}(R) \\ & \times \left(\mathbf{A}_k(R)\hat{\mathbf{M}}(R, k) - \mathbf{B}_k(R)\right), \end{aligned} \quad (8)$$

[1] We use the notation $v = v_2$, $v' = v_3$ and $v'' = v_4$ for simplicity

where R is the upper limit in the variable-phase equation,

$$\mathbf{A}_k(r) = \text{diag}\left(\frac{\hat{j}_{l_1}(kr)}{k^{l_1+1}}, \dots, \frac{\hat{j}_{l_N}(kr)}{k^{l_N+1}}\right), \quad (9)$$

$$\mathbf{B}_k(r) = \text{diag}\left(\hat{y}_{l_1}(kr)k^{l_1}, \dots, \hat{y}_{l_N}(kr)k^{l_N}\right), \quad (10)$$

and $\mathbf{U}(R)$ is the reduced potential matrix. These are coupled non-linear differential equations which may become stiff in the presence of singularities in which case many integration points would be needed. For a discussion of these equations and their singularities in connection to the renormalization group and their fixed point structure see Refs. [35, 36, 37].

Table 1: Low-energy scattering parameters for the $^3S_1$ eigen-phase. We quote the numbers of Ref. [41] for the PWA [15] and the Nijm-I, Nijm-II and Reid 93 potentials [16], (first four rows), our results integrating the discrete variable S-matrix equations with $N = 2 \times 10^5$ grid points for the Nijm-II and Reid 93 [16] and AV18 [17] potentials quoting numerical uncertainties (in boldface) relative to the computation with $N = 1 \times 10^5$. Statistical errors are also quoted when available.

	α_0	r_0	v_2	v_3	v_4
PWA	5.420(1)	1.753(2)	0.040	0.672	−3.96
Nijm I	5.418	1.751	0.046	0.675	−3.97
Nijm II	5.420	1.753	0.045	0.673	−3.95
Reid93	5.422	1.755	0.033	0.671	−3.90
NijmII	5.4197(**3**)	1.75343(**3**)	0.04545(**1**)	0.6735(**1**)	-3.9414(**8**)
Reid93	5.4224(**2**)	1.75550(**3**)	0.03269(**1**)	0.6721(**1**)	- 3.8867(**7**)
AV18	5.4020(**2**)	1.75171(**3**)	0.03598(**1**)	0.6583(**1**)	-3.8507(**7**)
DS-OPE	5.435(2)	1.774(3)	0.055(1)	0.650(2)	−3.84(1)
DS-TPE	5.424	1.760	0.050	0.666	−3.90
G-OPE	5.441	1.781	0.056	0.642	−3.80

[h]

3

Table 2: Low energy threshold np parameters for all partial waves with $j \leq 5$. The central value and *statistical* error bars are given on the first line of each partial wave and correspond to the mean and standard deviation of a population of 1020 parameters calculated with the Monte Carlo family of potential parameters described in [26] using the DS-OPE potential [20, 21]. The second line quotes the *systematic* uncertainties, the central value and error bars correspond to the mean and standard deviation of the 6 realistic potentials Ni-jmII [16], Reid93 [16], AV18 [17], DS-OPE [20, 21], DS-χTPE [22, 23] and Gauss-OPE [24]. For each partial wave we show the scattering length α and the effective range r_0, both in $\mathrm{fm}^{l+l'+1}$, as well as the curvature parameters v_2 in $\mathrm{fm}^{l+l'+3}$, v_3 in $\mathrm{fm}^{l+l'+5}$ and v_4 in $\mathrm{fm}^{l+l'+5}$. For the coupled channels we use the nuclear bar parameterization of the S matrix. Uncertainties smaller than 10^{-3} are not quoted

Wave	α	r_0	v_2	v_3	v_4
$^1S_0$	−23.735(6)	2.673(9)	−0.50(1)	3.87(2)	−19.6(1)
	−23.740(6)	2.69(3)	−0.48(1)	3.6(1)	−19.4(6)
$^3P_0$	−2.531(6)	3.71(2)	0.93(1)	3.99(3)	−8.11(5)
	−2.6(2)	3.6(5)	0.8(6)	3.9(1)	−8.4(10)
$^1P_1$	2.759(6)	−6.54(2)	−1.84(5)	0.41(2)	8.39(9)
	2.77(3)	−6.5(1)	−1.7(2)	0.5(3)	8.1(3)
$^3P_1$	1.536(1)	−8.50(1)	0.02(1)	−1.05(2)	0.56(1)
	1.53(1)	−8.55(8)	−0.02(4)	−1.0(2)	0.3(4)
$^3S_1$	5.435(2)	1.852(2)	−0.122(3)	1.429(7)	−7.60(3)
	5.42(1)	1.84(1)	−0.132(8)	1.44(1)	−7.65(6)
ϵ_1	1.630(6)	0.400(3)	−0.266(5)	1.47(1)	−7.28(2)
	1.62(2)	0.40(1)	−0.27(1)	1.46(2)	−7.30(4)
$^3D_1$	6.46(1)	−3.540(8)	−3.70(2)	1.14(2)	−2.77(2)
	6.44(4)	−3.56(2)	−3.76(5)	1.09(4)	−2.7(1)
$^1D_2$	−1.376	15.04(2)	16.68(6)	−13.5(1)	35.4(1)
	−1.380(7)	15.0(1)	16.6(2)	−13.1(3)	36.1(16)
$^3D_2$	−7.400(4)	2.858(3)	2.382(9)	−1.04(2)	1.74(2)
	−7.40(1)	2.861(8)	2.40(2)	−0.98(3)	1.8(1)
$^3P_2$	−0.290(2)	−8.19(1)	−6.57(5)	−5.5(2)	−12.2(3)
	−0.287(6)	−8.2(2)	−6.6(7)	−5.3(18)	−11.7(24)
ϵ_2	1.609(1)	−15.68(2)	−24.91(8)	−21.9(3)	−64.1(7)
	1.607(6)	−15.7(2)	−25.0(7)	−21.9(30)	−63.6(69)
$^3F_2$	−0.971	−5.74(2)	−23.26(8)	−79.5(4)	−113.0(16)
	−0.970(5)	−5.7(1)	−23.1(6)	−79.0(35)	−113.0(129)
$^1F_3$	8.378	−3.924	−9.869(4)	−15.27(2)	−1.95(7)
	8.376(7)	−3.927(5)	−9.89(3)	−15.4(2)	−2.3(4)
$^3F_3$	2.689	−9.978(3)	−20.67(2)	−19.12(8)	−27.7(2)
	2.692(7)	−9.97(3)	−20.6(1)	−19.0(4)	−27.0(7)
$^3D_3$	−0.134	1.373	2.082(3)	1.96(1)	−0.45(3)
	−0.15(2)	1.370(3)	2.07(2)	1.91(7)	−0.5(1)
ϵ_3	−9.682	3.262	7.681(3)	9.62(2)	−1.09(5)
	−9.684(6)	3.258(5)	7.66(3)	9.5(1)	−1.2(2)
$^3G_3$	4.876	−0.027	0.019(2)	0.07(1)	−2.69(3)
	4.875(3)	−0.04(1)	−0.03(6)	−0.2(3)	−3.1(6)
$^1G_4$	−3.208	10.833(1)	34.629(9)	83.04(8)	108.1(4)
	−3.213(8)	10.81(2)	34.54(8)	82.5(4)	106.1(17)
$^3G_4$	−19.145	2.058	6.814	16.769(4)	10.00(2)
	−19.15(1)	2.058(1)	6.814(4)	16.78(2)	10.05(7)
$^3F_4$	−0.006	−3.043	−4.757(1)	73.903(5)	662.21(9)
	−0.009(3)	−3.040(8)	−4.75(5)	74.0(4)	662.5(40)
ϵ_4	3.586	−9.529	−37.02(3)	−184.40(2)	−587.28(9)
	3.590(9)	−9.53(2)	−37.02(7)	−184.5(3)	−586.4(19)
$^3H_4$	−1.240	−0.157(2)	−1.42(1)	−14.0(1)	−99.0(9)
	−1.241(4)	−0.17(1)	−1.51(9)	−14.9(9)	−105.4(59)
$^1H_5$	28.574	−1.727	−7.906	−32.787	−59.361
	28.58(2)	−1.727	−7.905(4)	−32.78(2)	−59.38(6)
$^3H_5$	6.081	−6.439	−25.228	−82.511(3)	−168.47(2)
	6.09(2)	−6.43(2)	−25.21(6)	−82.5(1)	−168.1(9)
$^3G_5$	−0.008	0.481	1.878	6.100	6.791
	−0.010(2)	0.480	1.878(1)	6.098(4)	6.78(1)
ϵ_5	−31.302	1.556	6.995	28.179	48.376(2)
	−31.31(2)	1.556	6.993(4)	28.17(1)	48.35(3)
$^3I_5$	10.678	0.011	0.146	1.441	6.546(6)
	10.680(6)	0.011	0.144(1)	1.43(2)	6.5(1)

For interactions which are smooth functions in configuration space $\mathbf{U}(r)$, we propose a particular integration method by making a delta-shell sampling of the interaction taking a sufficiently small Δr. For simplicity we assume equidistant points $r_i = i\Delta r$ with $i = 1, \ldots, N$ and a maximum interaction radius $r_{\max} = N\Delta r$ which corresponds to a delta-shells representation

$$\bar{\mathbf{U}}(r) = \sum_i \mathbf{U}(r_i)\delta(R - r_i)\Delta r. \tag{11}$$

Actually, when substituting a DS potential, $\mathbf{U}(R) = \sum_i \Lambda_i \delta(R - r_i)$, in Eq. (8) a recurrence relation is obtained between the value of the $\hat{\mathbf{M}}$ on the left and right side of each concentration radii r_i. That was the method used in Ref. [29]. In practice, it is numerically better to solve the Schrödinger equation and matching logarithmic derivatives piecewise as done in [21], yielding to

$$\hat{\mathbf{M}}(r_{i+\frac{1}{2}}, k) - \hat{\mathbf{M}}(r_{i-\frac{1}{2}}, k) = \left(\hat{\mathbf{M}}(r_{i+\frac{1}{2}}, k)\mathbf{A}_k(r_i) - \mathbf{B}_k(r_i)\right)$$
$$\times \Lambda_i \left(\mathbf{A}_k(r_i)\hat{\mathbf{M}}(r_{i-\frac{1}{2}}, k) - \mathbf{B}_k(r_i)\right). \tag{12}$$

Taking the low energy expansion of Eq. (3) with the corresponding ones for $\mathbf{A}_k$ and $\mathbf{B}_k$

$$\mathbf{A}_k = \mathbf{A}_0 + \mathbf{A}_2 k^2 + \mathbf{A}_4 k^4 + \ldots \tag{13}$$
$$\mathbf{B}_k = \mathbf{B}_0 + \mathbf{B}_2 k^2 + \mathbf{B}_4 k^4 + \ldots \tag{14}$$

it is possible to obtain a recurrence relation for each matrix in Eq. (3). The first two lowest order expansions are given by

$$-\mathbf{a}_{i+\frac{1}{2}}^{-1} + -\mathbf{a}_{i-\frac{1}{2}}^{-1} = \left(\mathbf{a}_{i+\frac{1}{2}}^{-1}\mathbf{A}_0 + \mathbf{B}_0\right)$$
$$\times \Lambda_i \left(\mathbf{A}_0 \mathbf{a}_{i-\frac{1}{2}}^{-1} + \mathbf{B}_0\right) \tag{15}$$

$$\mathbf{r}_{i+\frac{1}{2}} - \mathbf{r}_{i-\frac{1}{2}} = -2\left(\mathbf{a}_{i+\frac{1}{2}}^{-1}\mathbf{A}_0 + \mathbf{B}_0\right)$$
$$\times \Lambda_i \left(\frac{1}{2}\mathbf{A}_0 \mathbf{r}_{i-\frac{1}{2}} - \mathbf{A}_2 \mathbf{a}_{i-\frac{1}{2}}^{-1} - \mathbf{B}_2\right)$$
$$- \left(\frac{1}{2}\mathbf{r}_{i+\frac{1}{2}}\mathbf{A}_0 - \mathbf{a}_{i+\frac{1}{2}}^{-1}\mathbf{A}_2 - \mathbf{B}_2\right)$$
$$\times \Lambda_i \left(\mathbf{A}_0 \mathbf{a}_{i-\frac{1}{2}}^{-1} - \mathbf{B}_0\right). \tag{16}$$

Note the hierarchy of the equations where low energy parameters to a given order involve the same or lower orders only. These recursive equations are reversible, i.e. going upwards or downwards are inverse operations of each other on the discrete radial grid. They appeared for S-waves in Ref. [38] for the scattering length and the effective range. The initial condition corresponds to taking a trivial solution,

$$\mathbf{a}_{-\frac{1}{2}} = \mathbf{r}_{-\frac{1}{2}} = \cdots = 0 \tag{17}$$

whereas the final value provides the sought low energy parameters

$$\mathbf{a} = \mathbf{a}_{N+\frac{1}{2}}, \qquad \mathbf{r} = \mathbf{r}_{N+\frac{1}{2}}, \qquad \cdots \tag{18}$$

A good feature of these discretized variable phase-like equations is that they jump over singularities. The calculation of the low energy threshold parameters with a DS potential is very similar to the calculation of phase-shifts detailed in the appendix B of [21] and is also the discrete analogous of the variable S matrix method of [29].

5. Sampling the NN interaction: Fine graining vs Coarse graining

Several high quality interactions stemming from 1993 Nijmegen PWA such as the NijmII, Reid93, AV18 potentials are smooth functions in configuration space. For the DVSM method this means that the values $U(r_i)$ are *given* for $U = U_{\text{NijmII}}, U_{\text{Reid93}}, U_{\text{AV18}}$, and thus a fine graining $\Delta r \rightarrow 0$ is needed. We test the numerical accuracy and precision of the approach by using a finite grid representation and determine the low energy parameters of these potentials. In particular, we take $r_{\max} = 100$fm and $\Delta r = 0.01, 0.005, 0.001, 0.0005$fm corresponding to $N = 1 \times 10^4, 2 \times 10^4, 10^5, 2 \times 10^5$ grid points respectively and convergence is established for both Δr and $r_{\max}$.

For illustration we show in Fig. 1 eye-ball convergence for $v_{2,3,4}$ (eigen) in the $^3S_1$ channel, which is achieved with an integration upper limit of $r_{\max} = 30 - 40$fm. Sufficiently high numerical convergence is comfortably obtained with $r_{\max} = 100$fm for all partial waves with $J \leq 5$.

In order to gauge the accuracy of our calculation we compare with the last revision of the Nijmegen group [41]. In table 1 we show our results computed with the DVSM method. As we see, our implementation allows for high numerical precision which can be tuned to be the highest one among other sources of uncertainties, namely statistical and systematic errors to be discussed below. If we take the quoted numbers in Ref. [41] as significant figures and assuming the standard round-off error rules their numerical error is smaller than a half of the last provided digit. Our results are mostly compatible with theirs but considerably more precise.

It is useful to ponder on our numerical accuracy by looking into other possible integration methods. In the conventional Numerov of Runge-Kutta methods, usually employed for smooth potentials, convergence is defined in terms of the precision of the wave function, so that one needs a large number of meshpoints. The accuracy is also an issue in momentum space calculations where the momentum grid has an UV cut-off Δp which requires large matrices to make the low energy limit precise.

Alternatively, as pointed out in our previous works, the *same* level of accuracy and precision with much less computational cost can be achieved by taking the $U(r_i)$ as fitting parameters themselves to NN scattering data (or pseudodata). This is the basic idea behind coarse graining, implicit in the work by Avilés [42] and exploited in Refs. [20, 21] as the DS-potential samples the interaction with an integration step fixed by the maximum resolution dictated by the shortest de Broglie wavelength, namely $\Delta r \sim 0.5$ fm. A further advantage as compared to more conventional methods is the numerical stability of the method, since the number of arithmetic operations required with a few delta shells avoids accumulation of round-off errors.

6. Statistical and Systematic Uncertainties

The uncertainty discussed in the previous section is purely of numerical character and does not reflect the physical accuracy inferred directly from the experimental data [20, 21] nor the dependence inherited from the model used to analyze the data.

Statistical uncertainties are presented in table 2 which shows the low energy np threshold parameters of all partial waves with $j \leq 5$ for the DS-OPE potential presented in [20, 21]. To propagate statistical uncertainties we use our recent Monte Carlo bootstrap to NN data [26], where the set of potential parameters is replicated 1020 times, and the mean and standard deviation provide the central value and 1σ confidence interval respectively. It is very important to note that even though the threshold parameters encode the low energy structure of the NN interaction the statistical uncertainties are propagated from scattering data up to 350MeV. This approach encodes the high accuracy of a full-fledged PWA into a model independent low energy representation featured by the ERE. As we see the statistical precision is very high. We note in passing that, compared to our analysis of the $^3S_1$-eigen channel, the Nijmegen group had about *half* the data but provided *twice* the statistical precision as we do (see Table 1). This apparent inconsistency could be due to the different error propagation method.

We turn now to estimate the systematic uncertainty. Even though several phenomenological potentials can reproduce their contemporary NN scattering database, discrepancies have been found when comparing their corresponding phase-shifts [39, 40]. These discrepancies account for the systematic uncertainties of the NN interaction, which reproduces the same data with different representations of the potential. Although the propagation of systematic uncertainties is not as direct as the statistical one, we observe that differences in phase-shifts tend to be at least an order of magnitude larger than the statistical error bars [22, 23, 24]. A similar trend is found when comparing scattering amplitudes and Skyrme coefficients or counterterms in different partial waves [25]. To estimate the systematic uncertainties of the NN interaction at low energies we take different realistic potentials and compare their low energy threshold parameters. Any estimate of the systematic errors based on variations of the potential form or possible radial dependences will provide a lower bound to the uncertainties. Besides the form of the potential used to fit the data, another source of systematic error is the selection of the data itself, which must be permanently questioned due to addition of possible future data. Thus, the changes from the 3σ-selected database of the Nijmegen analysis 20 years ago comprising $N = 4313$ np and pp scattering data [15] to our recent 3σ-self-consistent database [20, 21] with about twice $N = 6713$ np and pp scattering data can be taken as an estimate on how much do we expect our predictions to change when a large body of new data is incorporated. Specifically we take six realistic local or minimally non-local potentials (i.e. containing L^2 dependences or quadratic tensor interactions) such as NijmII [16], Reid93 [16], AV18 [17], which provided a $\chi^2/$d.o.f ~ 1 to the Nijmegen database [15], and the new DS-OPE [20, 21], DS-χTPE [22, 23] and Gauss-OPE [24] which also provide a $\chi^2/$d.o.f ~ 1 to the Granada database [21]. To stress the obvious, we associate the increase of about 3400 np and pp data from the Nijmegen to the Granada database with an additional systematic error, foreseeing the possible impact that additional new data might have in

the future [2]. The values for the NijmII [16], Reid93 [16] have been determined already [29], whereas the remaining ones are determined here. Our results are presented in Table 2 (second line of each partial wave) which shows the mean and standard deviation of the low energy threshold parameters of the six local potentials. Comparison of the errors quoted in Table 2 clearly shows that the main uncertainty in the low energy parameters is due to the different representations or choices of high quality potential and not to the propagation of experimental uncertainties used to fix the most-likely potential chosen for the least squares χ^2-analysis.

Our conclusions are vividly illustrated in Fig. 1. As we see the spread of all potential results is larger than the statistical error band, which is our main point.

7. Conclusions

To summarize, we have calculated the low energy threshold parameters of the coupled channel effective range expansion for all partial waves with $j \leq 5$ by using a discrete version of the variable S-matrix method. This approach provides satisfactory numerical precision at a low computational cost, qualifying as a suitable method to compare statistical vs systematic errors. Statistical uncertainties are propagated via the bootstrap method [26] where a family of DS-OPE potential parameters is fitted after experimental data are replicated. We also made a first estimate of the systematic uncertainties of the NN interaction by taking six different realistic potentials (i.e. with $\chi^2/\mathrm{d.o.f} \lesssim 1$) and calculating the low energy threshold parameters with each of them. These estimates should be taken as a lower bound. In accordance with preliminary estimates [39, 40], the systematic uncertainties tend to be at least an order of magnitude larger than the statistical ones. The present results encode the full PWA at low energies and have some impact in *ab initio* nuclear structure calculations in nuclear physics. They could also be used as a starting point to the determination and error propagation of low energy interactions with the proper long distance behavior in addition to the universal One Pion Exchange interaction.

References

[1] H. Bethe, Phys.Rev. **76**, 38 (1949).

[2] L. Puzikov, R. Ryndin, and J. Smorodinsky, Nuclear Physics **3**, 436 (1957).

[3] C. R. Schumacher and H. A. Bethe, Physical Review **121**, 1534 (1961).

[4] R. Alvarez-Estrada, B. Carreras, and M. Goñi, Nuclear Physics B **62**, 221 (1973).

[5] J. Bystricky, F. Lehar, and P. Winternitz, J.Phys.(France) **39**, 1 (1978).

[6] H. Kamada, W. Glöckle, H. Witała, J. Golak, and R. Skibiński, Few-Body Systems **50**, 231 (2011).

[7] K. Chadan and P. C. Sabatier, *Inverse problems in quantum scattering theory* (Springer Publishing Company, 2011).

[8] S. Okubo and R. Marshak, Annals of Physics **4**, 166 (1958).

[9] J. Dudek, B. Szpak, B. Fornal, and A. Dromard, Physica Scripta **2013**, 014002 (2013).

[10] J. Dobaczewski, W. Nazarewicz, and P.-G. Reinhard, J.Phys. **G41**, 074001 (2014), 1402.4657.

[11] D. Ireland, and W. Nazarewicz (Guest Editors), J.Phys. **G**, *Special issue: Enhancing the interaction between nuclear experiment and theory through information and statistics (ISNET)* (2015) (in press).

[12] H. P. Stapp, T. J. Ypsilantis, and N. Metropolis, Phys. Rev. **105**, 302 (1957).

[13] R. Machleidt and G.-Q. Li, Phys.Rept. **242**, 5 (1994).

[14] J.R. Taylor, *An Introduction to Error Analysis: The Study of Uncertainties in Physical Measurements (2nd ed.)* (University Science Books, 1997).

[15] V. Stoks, R. Kompl, M. Rentmeester, and J. de Swart, Phys.Rev. **C48**, 792 (1993).

[16] V. Stoks, R. Klomp, C. Terheggen, and J. de Swart, Phys.Rev. **C49**, 2950 (1994), nucl-th/9406039.

[17] R. B. Wiringa, V. Stoks, and R. Schiavilla, Phys.Rev. **C51**, 38 (1995), nucl-th/9408016.

[18] R. Machleidt, Phys.Rev. **C63**, 024001 (2001), nucl-th/0006014.

[19] F. Gross and A. Stadler, Phys.Rev. **C78**, 014005 (2008), 0802.1552.

[20] R. Navarro Pérez, J. E. Amaro, and E. Ruiz Arriola, Phys.Rev. **C88**, 024002 (2013), 1304.0895.

[21] R. Navarro Pérez, J. E. Amaro, and E. Ruiz Arriola, Phys.Rev. **C88**, 064002 (2013), 1310.2536.

[22] R. Navarro Pérez, J. E. Amaro, and E. Ruiz Arriola, Phys.Rev. **C89**, 024004 (2014), 1310.6972.

[23] R. Navarro Perez, J. Amaro, and E. Ruiz Arriola, Few Body Syst. **55**, 983 (2014), 1310.8167.

[24] R. Navarro Pérez, J. E. Amaro, and E. Ruiz Arriola, Phys.Rev. **C89**, 064006 (2014), 1404.0314.

[25] R. Navarro Pérez, J. E. Amaro, and E. Ruiz Arriola, Jour. Phys. G (in press) (2014), 1406.0625.

[26] R. Navarro Perez, J. Amaro, and E. Ruiz Arriola, Phys.Lett. **B738**, 155 (2014), 1407.3937.

[27] R. N. Perez, E. Garrido, J. Amaro, and E. R. Arriola, Phys.Rev. **C90**, 047001 (2014), 1407.7784.

[28] F. Calogero, *Variable phase approach to potential scattering* (Elsevier, 1967).

[29] M. Pavon Valderrama and E. Ruiz Arriola, Phys.Rev. **C72**, 044007 (2005).

[30] E. Ruiz Arriola, arXiv:1009.4161 [nucl-th].

[31] M. Pavon Valderrama, Phys. Rev. C **84**, 064002 (2011) [arXiv:1108.0872 [nucl-th]].

[32] B. Long and C. J. Yang, Phys. Rev. C **84**, 057001 (2011) [arXiv:1108.0985 [nucl-th]].

[33] B. Long and C. J. Yang, Phys. Rev. C **85**, 034002 (2012) [arXiv:1111.3993 [nucl-th]].

[34] S. Elhatisari and D. Lee, Eur. Phys. J. A **48**, 110 (2012) [arXiv:1206.1207 [nucl-th]].

[35] M. Pavon Valderrama and E. Ruiz Arriola, Phys.Lett. **B580**, 149 (2004), nucl-th/0306069.

[36] M. Pavon Valderrama and E. Ruiz Arriola, Phys.Rev. **C70**, 044006 (2004), nucl-th/0405057.

[37] M. Pavon Valderrama and E. Ruiz Arriola, Annals Phys. **323**, 1037 (2008), 0705.2952.

[38] D. Entem, E. Ruiz Arriola, M. Pavon Valderrama, and R. Machleidt, Phys.Rev. **C77**, 044006 (2008), 0709.2770.

[39] R. Navarro Pérez, J. E. Amaro, and E. Ruiz Arriola (2012), 1202.6624.

[40] R. Navarro Pérez, J. E. Amaro, and E. Ruiz Arriola, PoS **QNP2012**, 145 (2012), 1206.3508.

[41] J. J. de Swart, C. P. F. Terheggen and V. G. J. Stoks, nucl-th/9509032.

[42] J. B. Aviles, Phys. Rev. C **6**, 1467 (1972).

---

²Note that the normality test foresees, within a confidence level, that when re-measurements of selected data are made, the statistical uncertainties will become smaller. It does not tell, however, what the error on interpolated energy or angle values would be. Thus new selected measurements will slightly change the most likely values for the parameters of the χ^2-fit.